Nano World Journal

https://doi.org/10.17756/nwj.2022-095

Review Article

Open Access

Experimental Investigation on Green Synthesis of Bimetallic Nanoparticles by Using Plant Extract: A Review

Preeti Bairwa and Vijay Devra*

Department of Chemistry, Janki Devi Bajaj Government Girls College, Kota, Rajasthan, India

***Correspondence to:**
Vijay Devra
Department of Chemistry
Janki Devi Bajaj Government Girls College
Kota, Rajasthan, India
E-mail: v_devra1@rediffmail.com

Received: December 23, 2021
Accepted: February 15, 2022
Published: February 17, 2022

Citation: Bairwa P, Devra V. Experimental Investigation on Green Synthesis of Bimetallic Nanoparticles by Using Plant Extract: A Review. *J Nanoworld* 8(1) 6-18.

Published by United Scientific Group

Abstract

The use of viable cells in the green production of nanoparticles (NPs) is a promising and unique method in nanotechnology. The purpose of this work was to provide a comprehensive dissection on the use of various extracts of plant parts in the synthesis of bimetallic nanoparticles (BMNPs). In comparison to the physical and chemical methods, green nanotechnology based on biosynthesis has recently attracted a lot of attention. Biosynthesis has been discovered to be more energy-efficient and capable of avoiding the usage of toxic chemicals. Several strategies have recently been employed to boost the productivity of NPs with varying sizes, shapes, and stability. The shape, size, surface charge, and surface area of NPs have all been associated with their mechanical, optical, magnetic, and chemical properties. The impact of various reaction conditions such as pH, plant extract concentration, reaction temperature, and ionic ratio on the synthesis of BMNPs was also discussed to provide a thorough knowledge of how these variables affect the development of BMNPs. Different techniques are used to detect and analyze biosynthesized NPs, such as UV–Vis spectroscopy, FT-IR, TEM, SEM, AFM, DLS, XRD, zeta potential studies, and so on. The green method of NPs synthesis can be used in a variety of biotechnological sectors.

Keywords

Green synthesis, Bimetallic nanoparticles, Experimental investigation, Characterization techniques

Introduction

Nanoscience is an interdisciplinary field of study that encompasses physics, chemistry, medicine, and materials science. Nanotechnology is sometimes referred to as a general-purpose technology since it will have a significant impact on practically every aspect of society and industry in its advanced form [1]. Norio Taniguchi of Tokyo University of Science coined the term "nanotechnology". The prefix 'Nano' derives from a Greek term that means "dwarf" and refers to objects that are one-billionth in size [2]. The study of structures and molecules in the nanometre range of 1-100 nm is known as nanotechnology [3]. Nanotechnology is a type of technology that is employed in practical applications such as devices. NPs are classified into many categories based on their size, shape, physical, and chemical characteristics. Metal NPs, carbon NPs, semiconductor NPs, ceramic NPs, polymeric NPs, and lipid-based NPs are just a few of them. Metal NPs have unique properties compared to their bulk metal counterparts, which have a degraded density of energy state and a high surface-to-volume ratio, boosting their contact with other molecules [4].

In both technological and scientific terms, BMNPs have received a lot of

interest compared to monometallic NPs because BMNPs have better capabilities [5] and alternative arrangements, such as nanoalloys and core-shells, can be created with unique surface features [6]. Different techniques for the synthesis of BMNPs have been devised. The top-down and bottom-up approaches are the two most frequent methodologies for particle synthesis [7]. The bulk material is broken down into small particles by size reduction in the top-down method, whereas NPs are produced by self-assembly of atoms into nuclei, which then develop into nano-sized particles in the bottom-up process (Figure 1) [8]. To synthesize NPs, a top-down approach has been used, which comprises physical and chemical processes such as hydrothermal, microwave, electrochemical, laser ablation, thermal breakdown, and lithography [9-14].

These methods have significant drawbacks, such as defective surface formation, high manufacturing costs, high energy consumption, and the use of eco-toxic chemicals, which are responsible for carcinogenicity, genotoxicity, and cytotoxicity [15-17], as well as being more capital intensive and yielding

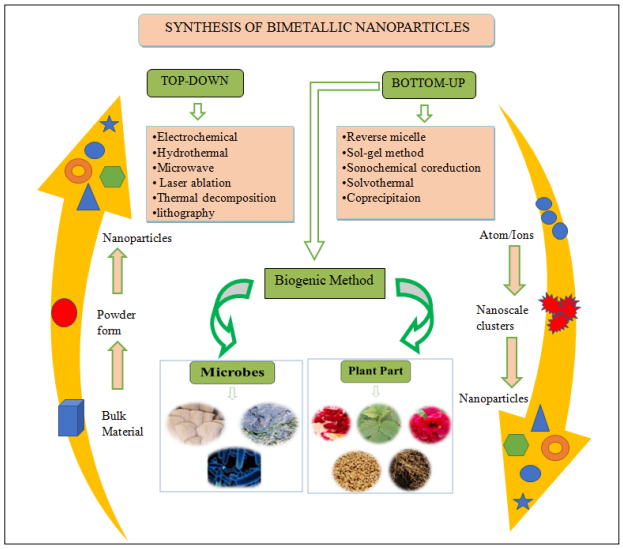

Figure 1: Synthesis methods of bimetallic nanoparticle.

lower nanoscale materials [18]. The bottom-up strategy, in which a NPs is created from simpler molecules recognized as reaction precursors, is the most successful way for NPs synthesis. Depending on the subsequent uses, adjustments in precursor quantities and reaction conditions such as pH temperature, etc. can be used to control the size and synthesis of NPs [8]. Several species serve as safe, eco-friendly, and green precursors in researchers' constant efforts to design a green approach to manufacture stable and well-defined functionalized NPs [19].

The green chemistry technique of plant NPs synthesis links nanotechnology with plant biotechnology. Thus, it is important to investigate NPs manufacturing, as well as themes of interest such as economic relevance, environmental friendliness, and social appropriateness, as well as the accessibility of local properties. Green synthesis is a bottom-up strategy in which a biological extract is employed to synthesize metallic NPs instead of a chemical reducing agent [20]. The use of an aqueous extract of natural resources such as plants, leaves, seeds, fruits, biomass, proteins, and starch as reducing and capping/stabilizing agents in the biosynthesis of metal NPs is considered an environmentally friendly, inexpensive, and simple alternative to physical and chemical methods [21]. Bimetallic nanostructures can be classified into two sorts of configurations: alloy and heterostructure.

Homogeneous and gradient alloys are two different types of alloyed bimetallic nanostructures. Atoms of the two metals are uniformly distributed throughout the structure in homogeneous alloys; the atom distribution can be either ordered (intermetallic) or statistically random [22]. There is clear segregation between the two metal components in heterostructure bimetallic nanomaterials. One of the most common examples is the core-shell structure, which is made up of a metal core and a shell made up of a different type of metal [23].

Green synthesis of BMNPs

Biological resources such as plant extract and microorganisms as bacteria, algae, fungi, viruses, and yeast as a reducing agent are used in the green synthesis. Microorganisms employed in biosynthesis require a culture media and aseptic conditions to thrive [24]. Plant extract is believed to be more useful than microorganisms due to its ease of production and availability [25]. Plants have a high inclination to generate nanoparticles since they are renewable, biodegradable, low-cost to handle, and provide NPs with a natural stabilizing agent immediately [26]. Flavonoids, proteins, polyphenols, amino acids, alkaloids, enzymes, reducing sugars, and a variety of other bioactive components found in plant extracts could be involved in the bio-reduction of metal ions to metal NPs and the stabilization/capping of the metallic NPs. The green synthesis of NPs is influenced by a variety of factors, including the parts of the plant, the solvent used for extraction, the pH of the solution, the salt concentration, and the reaction temperature [27], and can have a wide range of applications in fields such as magnetic devices, photocatalysis, microelectronic devices, anticorrosive coatings, biomedical, electrocatalysts, and also in powder metallurgy [19]. Plant materials such as leaves, bark, roots, stems, fruits, pericarp, seeds, latex [28-35], and secondary metabolites are used to synthesize different BMNPs (Figure 2). An aqueous solution of a suitable metal precursor is combined with a biological extract in the needed ratio to fabricate NPs. Stirring and heating can both initiate reactions. At room temperature, spontaneous reactions can occur in some instances [36]. The following two processes are used to make BMNPs from precursor salts: 1) Reduction and 2) Coreduction [22], which results in an alloy, mixed, or core-shell BMNPs being formed. The metal salts are added one by one in the first technique to extract so that the metal precursor generates nuclei on which the second metal precursor produces core-shell BMNPs. When metal precursors are introduced to the extract at the same time, the reduction of the metal ion that happens first and the metal ion that occurs later is determined by its reduction potential. This method results in an alloy or a mixture of BMNPs [37].

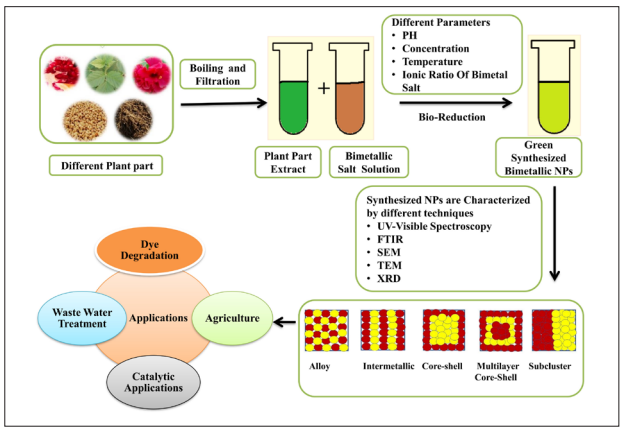

Figure 2: Green synthesis of bimetallic nanoparticles by plant extract.

Leaf extract

Using various plant leaf extracts, many studies have demonstrated the green production of BMNPs. For the production of Cu-Ag BMNPs, Al-haddad et al. [28] used leaf extract from the date palm tree (*Phoenix dactylifera*) as capping and reducing reagent. The use of Sidr leaves (*Ziziphus jujube*) extract to reduce the average bimetallic particle size to 26 nm was innovative in this study. The size of the produced BMNPs was measured in solution for both samples with and without capping reagent. In the presence of a capping reagent, the average particle size was reduced considerably from 1276 nm to 778 nm. The presence of flavonoid and phenolic components in Sidr leaves extract was responsible for the size reduction reported by Zaleska-Medynska et al. [22]. Another study published by Rosbero et al. [38] used aqueous leaf extracts of *Carica papaya* as a reducing agent in the production of Ag-Cu NPs. Canini et al. [39] used GC-MS to quantify the secondary metabolites found in *Carica papaya* leaf extracts, finding seven phenolic compounds including quercetin, protocatechuic acid, p-coumaric acid, caffeic acid, chlorogenic acid, kaempferol, and 5,7-dimethoxycoumarin. *Carica papaya* secondary metabolites are capable of efficiently reducing metal ions and promoting their subsequent stability. They discovered a star-like structure with a hydrodynamic size of 420.7 nm (DLS) and a TEM size of 150 nm. The sample is crystalline, according to XRD examination, with diffraction peaks corresponding to Ag, Ag_2O, and CuO. The synthesized NPs degraded chlorpyrifos effectively in water, yielding less hazardous breakdown products such as 3, 5, 6-trichloro-2-pyridinol, and Diethyl thiophosphate Akinsiku et al. [40] use an aqueous leaf extract of an indigenous *Senna occidentalis* (coffee Senna). For the synthesis of pseudocubic Ag-Ni NPs. Bioactive agents were found in the water and methanolic extracts of coffee Senna leaves, according to the solvent extraction data. Secondary metabolites glycosides and carbohydrates were detected in the water extract, which was responsible for metal bioreduction, whereas additional groups, such as tannins, phenols, flavonoids, and alkaloids, were detected in the methanolic extract of the same plant; these additional groups were probably more methanol soluble, and this was the putative reason for not detecting them in the pure water solvents. Gopinath et al. [41] studied the antibacterial and antibiofilm capabilities of *Gloriosa superba* aqueous leaf extract in the manufacture of Ag-Au nanoalloy against Gram-positive and Gram-negative bacteria. The stretching of C-O -C-O-C causes the 1259 and 1070 cm^{-1} bands to appear in the FT-IR spectra. The leaf extract's primary components are responsible for the observed reduction as well as the completion of the nanoparticle biosynthesis process. The band in the 1259 cm^{-1} spectra disappeared once the synthesis process was completed, demonstrating that the glycosides and water-soluble tannins present in the leaf extract aided in the reduction of metal ions to metal NPs. They observed that the BMNPs had a more efficient antibacterial activity effect on *Bacillus subtilis* than individual NPs. This was proposed to be due to the synergistic effect of the metals.

Verma et al. [42] investigated the use of *Ananas comosus* leaves extract as a reducing and stabilizing agent in the manufacture of Au-Ag core-shell NPs and their catalytic potency for the reduction of 4-nitrophenol to 4-aminophenol in 15 minutes for the first time. The DLS spectra show the 65 nm Z-average diameter of core-shell NPs with a polydispersed index (PDI) of 0.311. The HR-TEM demonstrates that Au-Ag NPs with sizes ranging from 5 to 10 nm have a spherical morphology. Alti et al. [43] were the first to report antileishmanial activity of alloy Ag-Au NPs employing three different herbal leaves (fenugreek, soybean, and coriander) in a single-step reduction method. With half-inhibitory concentrations (IC_{50}) in the range of 0.03 - 0.35 g/mL, all of the synthesized BMNPs had strong antileishmanial activities against promastigotes. Another study Lagashetty et al. [44] used piper beetle leaf extract as a reducing agent in the production of BMNPs. The XRD results of the produced NPs demonstrate that the AgNPs have peaks of diffraction signals at (100), (220), and (311) facets, whereas the AuNPs have signals at (111) and (200). Ag (JCPDS file 87–0720) and Au (JCPDS file 04–0784) d-spacing valuesare observed as in the pattern (Figure 3). Luo et al. developed a green synthesis of Fe-Pd NPs utilizing grape leaf aqueous extract and its catalytic application to remove Orange II [45]. Because Pd as a catalyst considerably reduced the activation energy of the process, they discovered that the synthesized BMNPs (98.0%) have a stronger ability to remove Orange II in 12 hours than Fe NPs (16.0%). Degradation ability is slightly lower (85.3%) than green generated Fe-Pd NPs when compared to chemically manufactured Fe-Pd NPs. This is because existing capping biomolecules not only prevented Fe

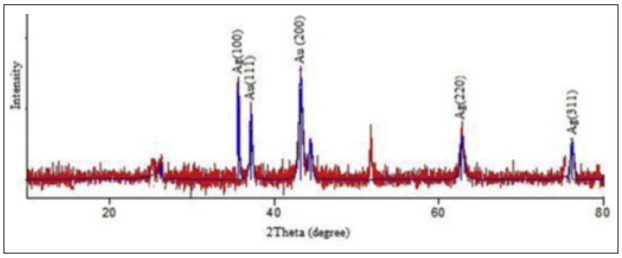

Figure 3: XRD Pattern of Ag-Ni Bimetallic Nanoparticles. (Credit-Lagashetty, A., &Ganiger, S. K. (2019). Synthesis, characterization, and antibacterial study of Ag–Au Bi-metallic nanocomposite by bioreduction using piper beetle leaf extract. Heliyon, 5(12), e02794)[44].

NPs from participating in the reaction before penetration but also improved stability, resulting in increased reactivity. Therefore, green produced Fe-Pd NPs, a longer reaction time and higher removal efficiency were reported when removing Orange II. In the presence of *Salvia officinalis* extract as a reducing and capping agent, Malik et al. [46] presented a one-pot seedless synthesis technique for the fabrication of core-shell Ag-Fe bimetallic nanoparticles. During the seedless reduction process, Ag^{+} ions were first reduced by reducing phytochemicals, such as polyphenols and flavonoids from aqueous extract of *Salvia officinalis* leaves, and then Fe^{3+} ions on the surface of Ag^{0}-seed were reduced according to their potential deposition.

Van Tien et al. produced Ag-Mn BMNPs for the first time utilizing *Arachispintoia* extract and co-reduction of silver nitrate and potassium permanganate (both leaves and stems) [47]. *Cycleapeltata* leaf extract was used by Suvrana et al. (2020) in recent work to synthesize Fe-Cu NPs. The fabrication of core-shell BMNPs with a size of 45 - 50 nm was established by investigation. This is the first report on the synthesis of bimetallic Fe-CuNPs and their possible use in the degradation of methyl green dye. Abdel-Aziz et al. [48] used *Ficus Benjamina* leaves to investigate the activity of zero-valent Fe-Cu BMNPs in removing carbamazepine from aqueous solutions. The BMNPs have a semi-spherical form with a size range of 19 – 63 nm, according to the results of the characterization. Table 1 summarizes some more recent findings on the manufacture of BMNPs by plant leaves.

Fruits and fruit latex extract

Certain scientists to synthesize BMNPs have recently used fruit and fruit latex (Table 2). Aqueous extract of *Kigelia Africana* fruits was used to synthesize Ag NPs and Ag-Cu NPs, according to Ashishie et al. [16]. The findings of the characterization show that Ag-Cu BMNPs generated from *K. Africana* are crystalline in form and are particularly effective at inhibiting *Staphylococcus aureus*. Both Ag NPs and Ag-Cu NPs showed a higher zone of inhibition (15 mm for Ag NPs and 13 mm for Ag-Cu NPs) against *Klebsiella pneumoniae* when compared to common antibiotics such ofloxacin, augmentin, ciprofloxacin, meropenem, or racinef, which were employed as controls in this investigation. For the synthesis of Cu-Ni BMNPs, Lamayi Danbature et al. use a fruit extract of the Palmyra palm as a green reducing agent [32]. The Optical characteristics, as well as the interaction between the generated Cu-Ni hybrid NPs and the raw fruit extract,are revealed by the characterization results of the synthesized NPs.

Adeyemi et al. used Kei apple fruit extract to investigate the production and cytotoxic characteristics of Au-Ag BMNPs [49]. Two bands (at a higher volume of plant extract) in the region of 458 and 560 nm appear as maxima in the absorption spectra as humps for the NPs (Au-Ag BMNPs), indicating core-shell behavior, while the observed peak at 540 nm confirms the alloy NPs (at a lower volume of extract), as supported by the TEM images. According to the study, the amount of fruit extract utilized had a significant impact on the particle size and shape of the NPs. Plant extracts with a lesser volume yield alloy NPs, while extracts with a higher volume yield core-shell NPs. Sundararajan and Pottail did another investigation employing *Artocarpus heterophyllus* fruit latex to synthesize Au-Ag BMNPs [35]. They looked at 15 nm spherical NPs, which had stronger antibacterial activity against the gram-negative strain *K. pneumonia* but were ineffective against all gram-positive pathogens. The crude latex extract is shown to be completely devoid of antibacterial activity. Adebayo et al. used *Persea Americana* (Avocado) fruit extract to synthesize ring-shaped Ag-Au alloy NPs with a size of 44 – 55 nm [50]. Protein molecules, amine, and hydroxyl groups were found to be responsible for particle stability and capping, according to FT-IR analyses. Antibacterial and antifungal activities have been discovered in NPs that have been synthesized.

Root extract

Recently, some studies reported to use root extract for synthesis of BMNPs (Table 2). Shehu et al. synthesize Ag-Ni BMNPs from *Borassusaethiopum* aqueous root extract [51]. They investigated the inhibitory activity of synthesized NPs against gram-negative- *Escherichia coli, Pseudomonas aeruginosa, K. pneumoniae*, and *Salmonella typhi* as well as gram-positive *Bacillus subtilus*. At 410 nm wavelength, the study finds surface plasmon resonance (SPR) of BMNPs. Using *Asparagus racemosus* root extract as a reducing agent, Amina et al. demonstrated antibacterial and immunomodulatory potentials of Ag-Au Alloy BMNPs [52]. Pure Ag and Au metal can be found in the Ag-Au alloy BMNPs matrix, according to EDX spectra. The immunomodulatory efficacy of the *A. racemosus* root extract, AgNPs, AuNPs, and Ag-Au alloy NPs is accomplish through measuring the cytokine levels in macrophages and NK cells of NK92 and THP1 cells using the solid-phase sandwich ELISA technique. The findings revealed that the *A. racemosus* root extract, AgNPs, and AuNPs can reduce pro-inflammatory cytokine levels in macrophages cells, whereas Ag-Au alloy NPs can lower cytokine responses in NK92 cells. When compared to single metal NPs and plant extract, alloy BMNPs have the greatest inhibitiory zone against *P. aeurgnosia* and Aureusstrains. Sharma et al. reported the synthesis of *Rheum emodi* roots extract mediated bimetallic Ag–Cu NPs with anticancer and antibacterial properties [53]. The discovery demonstrated the encapsulation of bioactive hydroxyl-anthraquinones on the surface of NPs as a capping, reducing, and stabilizing agent is revealed by FT-IR findings. Synthesized NPs have a powerful anti-cancer effect in breast (MDA-MB-231) cancer cell lines. Furthermore, the produced NPs have outstanding antibacterial activity against the pathogens *E. coli* and *S. aureus*, owing to the intrinsic hydroxy and phenol capping, which facilitates entry into the bacterial cell. Danbature et al. reported on the environmentally friendly synthesis of Ag-Co hybrid NPs from the aqueous root extract of palmyra and their larvicidal efficacy [30]. The maximum absorption wavelength was observed at 420 nm using a UV-Vis Spectrophotometer. Secondary metabolites found in the root extract of the Palmyra palm were responsible for metal reduction, according to FT-IR spectroscopy.

Flower extract

Currently different flower extracts are used for the synthesis of BMNPs (Table 2). Sarangapany and Mohanty synthesized bimetallic Au-Pt NPs anchored on TiO_2 nanocom-

Table 1: The green synthesis of bimetallic nanoparticles using different plant leaf extracts.

S.No.	Plant and source	Bimetallic nanoparticles	Characterization results		Applications	Reference
			TEM and SEM (morphology)	UV-Visible Spectroscopy(λ_{max})		
1	*Cassia tora* leaf extract	Au-Ag	7 - 27 nm, Spherical, Hexagonal Triangular	400 nm	-	[5]
2	Cyclea peltata leaf extract	Fe-Cu	45 - 50 nm, Spherical	250 nm	Dye degradation	[34]
3	Date palm tree *(Phoenix dactylifera)* leaves	Cu-Ag	778 nm, Semi-spherical agglomerated clusters	-	Catalytic activity	[38]
4	*Senna occidentalis* Leaf Extract	Ag-Ni	3 – 24 nm, Pseudo cubic	330 nm	Medical purpose	[40]
5	*Gloriosa superba* aqueous leaf extract	Au–Ag	10 nm, Spherical	559 nm	Antibacterial and antibiofilm activities	[41]
6	*Ananas comosus* leaves extract	Au-Ag	5 - 10 nm, Spherical	409 nm	Catalytic activity	[42]
7	Fenugreek leaf extracts	Au-Ag	10 - 12 nm, Spherical	541 nm	Antileishmanial activity	[43]
	Soybean leaf extracts	Au-Ag	10 - 12 nm, Spherical	533 nm	Antileishmanial activity	
	Coriander leaf extracts	Au-Ag	10 - 12 nm, Spherical	522 nm	Antileishmanial activity	
8	*Salvia officinalis* aqueous leaf extract	Ag–Fe	30 nm, Spherical	352 nm	Catalytic capability	[46]
9	*Ficus Benjamina* leaves	Fe-Cu	19 – 63 nm, Semi-spherical	-	Remove carbamazepine from the aqueous medium	[48]
10	*Aerva Lanata* leaf extract	Ag-Co	30 - 100 nm , Spherical	441 nm	Degradation of malachite green dye by irradiation under sunlight in optimum conditions	[79]
11	Eucalyptus leaf extract	Fe-Ni	20 – 50 nm, spherical and irregular shaped nanoparticles	-	Used to degrade methyl orange	[80]
12	Aqueous leaf extracts of *Majorana hortensis*	Ag-Cu	10 nm, Spherical	-	Antibacterial activities	[81]
13	*Cannabis sativa* leaf extract	Au–Ag	6.66 nm, Spherical	538 nm	Antibacterial activities	[82]
14	Lemon grass leaves extract	Au-Ag	~18 nm, Spherical	540 nm (Alloy),430 nm and 580 nm(Core-Shell)	Catalytic performance	[74]
15	Citrus lemon leaf extract	Au–Pd	~ 9.63 ± 3.95 d.nm , Polydisperse spherical	475 - 625 nm	Toxic mosquito larvicidal activity	[83]
16	*Phragmites Australis* aqueous leaf extract	Au-Pt	~35.1 ± 2.71nm, flower-like	572 nm	Cytotoxic activity	[84]
17	*StigmaphyllonOvatum* leaf	Ag-Au	14.9 nm, Triangular	542 nm	Cytotoxic potency	[85]

posite using dahlia flower extract through a greener approach [54]. The produced NPs were found to be effective in reducing organic contaminants. In a comparison of pristine (TiO_2, Fe_3O_4,Fe_3O_4@TiO_2) and monometallic (Fe_3O_4@TiO_2eAu, Fe_3O_4@TiO_2ePt) NPs, bimetallic (Fe_3O_4@TiO_2eAuPt)NPs demonstrated greater catalytic and recyclability efficiency towards organic pollutants reduction due to the synergistic effect of metal alloy and strong interaction of Au-Pt over the surface of TiO_2. Sharma et al. have been the first to use an aqueous extract of clove buds to make alloy Au-Ag BMNPs [55]. Clove buds are aromatic dried flower buds that are used as traditional medicine in India. It has antioxidant, antibacterial, antiviral, antiseptic, and anti-inflammatory properties, which is mainly because of the presence of Eugenol and other phenolic compounds reported by Cortés-Rojas et al. [56]. The NPs were primarily reduced and stabilized by flavonoids and eugenol. The development of hexagonal and polygonal BMNPs with a mean particle size of 16.04 nm is confirmed by electron microscopy. Biosynthesized NPs were found to have higher catalytic effectiveness for the degradation of methyl orange, methylene blue, and the reduction of p-nitrophenol in the study. Jeevarathinam et al. also used the *Crescentia alata* aqueous flower extract to synthesize bimetallic Ag-Au NPs [57]. The TEM analysis showed that spherical shapes of NPs with

an average size of 10 nm, high antibacterial, and antibiofilm activities towards Gram-positive and Gram-negative bacteria.

Bark extract

Bark extract is also used for the synthesis of different BMNPs (Table 2). Venkateswara Rao et al. produced Ag-Cu BMNPs with a size range of 80 - 90 nm using red sanders powder extract as a reducing agent and shown antibacterial activity [58]. Proteins, glucose, and other compounds in red sanders extract act as capping agents for the produced metal NPs, while flavonoids and sugars act as reducing agents. Karthika et al. also employed the bark extract *Guazuma ulmifolia* L. to synthesize Ag-Au alloy NPs with sizes ranging from 10 to 20 nm [59]. UV–Vis spectroscopy distinctive peaks at 510 nm confirmed the production of NPs. The catalytic activity of the synthesized NPs were demonstrated by their ability to reduce two organic dyes, 4-nitrophenol and congo red. The green produced NPs exhibit good DNA binding ability, according to fluorescence spectroscopy. Monometallic NPs have less binding activity than alloy NPs. In the UV-Vis absorption study, the binding constants of Ag, Au, and alloy NPs with DNA were 1. 18104, 1. 83104, and 2. 91104 M^{-1}, respectively. Mishra et al. synthesized the Fe, Pd, and Fe–Pd BMNPs using an aqueous bark extract of *Ulmus davidiana* and their application as magnetically recoverable catalysts for the [3 + 2] cycloaddition of 1,4-naphthoquinones or benzoquinones with β-ketoamides. UV, FTIR, and TGA measurements revealed that the polyols in the extract were responsible for reducing and capping the NPs [60]. An external magnetic field was employed to easily recover the produced BMNPs, which were subsequently reused with no loss of catalytic activity.

Seed extract

For the manufacture of spherical Au-Ag bimetallic nanocomposite, Gopalakrishnan et al. used *Silybum marianum* seed extract as a reducing and stabilizing agent [61]. It is worth noting that the seed extract was used for the green production of these NPs at room temperature. In the presence of the reducing agent sodium borohydride, they found that the produced nanocomposite acts as an efficient homogeneous catalyst in the degradation of 4-nitrophenol to 4-aminophenol. Sharma et al. created 34 – 66 nm Au–Ag BMNPs coated with flavonoids derived from the seed extract of the plant *Madhuca longifolia* for wound healing bioefficacy enhancement [62]. The aqueous-alcoholic extract of the seed (49.78%) of the plant *Madhuca longifolia* has wound healing bio-efficacy. Liquid ch-8030 analysis was used to determine the presence of seven flavonoids in the plant's seed extract. The flavonoids were crucial in the reduction and capping of Nps during biofabrication. The SPR band Au–Ag Nps at 470 nm was confirmed by UV–Vis spectroscopy. Mallikarjuna et al. used Fenugreek seed to synthesize Au-Pd Nps with sizes ranging from 200 to 500 nm and demonstrated catalytic activity of the nanostructures for the heterogeneous hydrogenation of 4-nitrophenol to 4-aminophenol in the presence of sodium borohydride [63]. The phytochemical polysaccharides found in fenugreek seeds help to reduce the ionic state of Au and Pd while also stabilizing the material and allowing for the creation of porous structures. The Au-Pd particles are generated along with the polysaccharide chains, rather than being entrapped in the gel networks, as revealed by SEM micrographs. Kumari et al. reported for the first time the synthesis of alloy and core-shell BMNPs at room temperature using pomegranate juice [64]. They investigated if increasing the Ag mole fraction in bimetallic nanostructures by changing the Au^{3+}/Ag^{+} ratio from 1:1 to 1:5 increased the Ag mole fraction. When the Au^{3+}/Ag^{+}ratio was 1:1, a core-shell configuration was observed, but when the amount of Ag^{+} was increased (Au^{3+}/Ag^{+}ratio of 1:2- 1:5), an alloyed configuration was formed (Table 2).

Bio-Wastes extract

The use of Bio waste of different plants are documented in Table 2. Newase et al. use banana peel extract powder for the synthesis of core-shell [65], Ag–Au nanocomposite. surface plasmon resonance results demonstrate that Ag–Au nanocomposite has a broad absorption peak at 500 nm, which is a characteristic of the material. Synthesize nanocomposite outperforms monometallic equivalents in terms of antibacterial and anti-biofilm properties. Ahmad et al. used *Trapa* peel extract to make Au-Ag NPs [66]. *Trapa* is a well-known Ayurvedic plant with antifungal, antibacterial, anti-inflammatory, and cancer-preventive properties. Because of the presence of the reducing sugar as well as the phenolic components present in the *Typhlonectes natans* peel, the synthesis of NPs from *Trapa* was faster than that reported from pomegranate waste. Synthesized NPs exhibited potential cytotoxic effects in various cancer cells. Ravikumar et al. first study the green synthesis of Ni-Fe NPs utilizing an ethanolic extract of *Punica granatum* (pomegranate) peels [67]. Antioxidant analysis and GC-MS results revealed that the extract included 2-furancarboxaldehyde 5-(hydroxymethyl), 1, 2-Di (2-furyl)-1,2-ethanedione, and 2,5 furan dicarboxaldehyde, which could contribute as reducing and stabilizing agents during synthesis. Wicaksono et al. used orange peel extract to synthesize Au-Pd core-shell NPs utilizing a two-step reduction technique [68]. The Au core NPs were synthesized using orange peel extract, while the Pd shell was generated by reducing the palladium chloride solution. The development of AuNPs at an optimum water/orange peel extract ratio of 16. 67 was indicated by a significant visible absorbance at 534 nm, whereas the formation of Au-Pd NPs was suggested by the disappearance of the peak at 534 nm. This research found that NPs generated employing a green synthesis method involving plant waste can be used as a good signal transducer in the development of colorimetric sensing methods.

Characterization Techniques

UV-Vis spectroscopy, Fourier-transform infrared spectroscopy (FT-IR), scanning electron microscopy/energy dispersive X-ray analysis (SEM/EDX), X-ray diffraction (XRD), and transmission electron microscopy (TEM) were used to characterize the produced NPs. The formation of NPs was indicated by UV-Vis and FT-IR methods, and the active components were adsorbed on the surface of the particles thereby stabilizing the NPs [7]. The property of functional groups or metabolites present on the surface of NPs, which may be responsible for NP reduction and stability, were investigated

Table 2: The green synthesis of bimetallic nanoparticles using different plant part (Fruit, Root, Flower, Bark, Seed, and Bio Waste).

S.No.	Plant and source	Bimetallic nanoparticles	Characterization Results		Applications	References
			TEM and SEM (morphology)	UV-Visible Spectroscopy(λ_{max})		
1	Root extract of Palmyra Palm	Ag-Co	-	420 nm	Potential control for larval population growth	[30]
2	Fruit extract of Palmyra palm	Cu-Ni	-	500 nm	Larvicidal activity	[32]
3	*Citrus Sinensis* (sweet orange) peels	Ag–Au	0.5 - 4 nm, Spherical	555 nm	Used to form nano-composite material	[33]
4	Kei-Apple (*Dovyalis caffra*) fruits	Ag- Au	9 – 14 nm, Core shell	540 nm	Anticancer behavior	[49]
5	Aqueous fruit latex extract of *Artocarpus Heterophyllus*	Ag–Au	15 nm, Spherical	552 nm	Antibacterial activity	[35]
6	Root extract of *Borassusa ethiopum*	Ag-Ni	-	410 nm	Antibacterial	[51]
7	*Asparagus Racemosus* root extract	Ag-Au	10 – 50 nm, Spherical	483 nm	Antibacterial and iiImmunomodu-latory	[52]
8	*Rheum emodi* roots extract	Ag–Cu	40 – 50 nm , Pseudo-spher-ical	422 nm	Antibacterial and anticancer	[53]
9	Dahlia flower extract	Au-Pt	63 nm, Spherical	-	-	[54]
10	Clove buds extract	Au-Ag	16.04 nm , Hexagonal and polygonal	535 nm	Antioxidant activity	[55]
11	*Crescentia alata* aqueous flower extract	Au-Ag	10 nm, Spherical	-	Antibacterial and antibiofilm activities	[57]
12	Red sanders powder extract	Ag-Cu	80 - 90 nm, Spherical	-	Antibacterial Activity	[58]
13	*Guazuma ulmifolia* bark	Au-Ag	10 - 20 nm, Spherical	510 nm	Photocatalytic, An-ticancer activity	[59]
14	Bark extract of *Ulmus davidiana*	Fe–Pd	Spherical	-	Catalytic activity	[60]
15	*Silybum Marianum* seed extract	Au–Ag	Spherical	500 nm	Homogeneous catalytic activity	[61]
16	Seed extract of *Madhuca longifolia*	Au–Ag	34 – 66 nm, Spherical	470 nm	Antimicrobial property	[62]
17	Fenugreek seeds	Au-Pd	200 - 500 nm, Spherical	320 nm	Catalytic activity	[63]
18	*Trapa* peel extract	Au-Ag	26 – 90 nm, Hexagonal,tri-angular, and spherical	~495 nm	Cytotoxicity	[66]
19	Orange peel extract	Au-Pd	Core diameter of 40 nm and an average shell thick-ness of 7 nm, Spherical	534 nm	Colorimetric sensing application	[68]
20	Palmyra Palm fruit extract	Cu-Co	-	500 nm	Larvicidal potential	[86]
21	Fruit pulp of *Moringa Oleifera*	Ag-Cu	9 nm , Spherical	290 nm	Antimicrobial activity.	[87]
22	Chinese Wolfberry fruit extract	Ag- Au	< 15 nm, Sphere-like	430 - 490 nm	Photocatalytic activity	[88]
23	*Plumbago zeylanica* root extract	Au–Ag	90 nm , Hexagonal	-	-	[89]
24	*Syzygium cumini* bark extract	Au-Ag	10 – 20 nm , Spherical	-	-	[89]
25	Turmeric (*Curcuma longa*) powder support	Ag–Cu	40 – 55 nm , Cluster	-	Catalytic reduction	[90]
26	Aqueous stem extracts of *Cissus quadrangularis* (“Haddjod”)	Cu-Zn	-	393 nm	-	[91]
27	Arachis pintoi extract (both leaves and stems)	Ag –Mn	3.3 nm, Spherical	-	Antibacterial activity	[47]
28	*Theobroma cacao* L. seeds extract	Pd-CuO	40 nm	-	Catalytic performance	[92]
29	Medicinal plant *Dioscorea bulbifera* tuber extract	Pt-Pd	2 - 25 nm, Spherical	420 nm	Anticancer and antioxidant activities	[93]

using FT-IR spectroscopy [69]. The morphology and size of the resulting NPs are clarified using TEM and SEM. XRD of nanomaterials provide a plethora of information, ranging from phase formation to crystallite estimation, cross-section strain to crystallographic introduction. XRD is non-contact and non-destructive, making it perfect for in situ research [70]. EDS and DLS are two further approaches for the characterization of NPs. EDS is used to isolate the characteristic X-rays of different elements into an energy spectrum, while DLS is used to identify the elemental composition of metal NPs. The surface charge and the hydrodynamic radius of NPs calculated using dynamic light scattering analysis of incident photons.

Factors influencing the green synthesis of bimetallic nanoparticles

BMNPs are often produced by mixing two different aqueous metal solutions with a plant extract as a reducing agent. Given the presence of two metal ions with distinct reduction potentials in a solution, a competitive reduction is expected in the production of BMNPs [71]. Modifying the sizes and shapes of metal nanoparticles appears to be compelled by environmental changes or influenced by functional molecules. Temperature, pH, incubation time, aeration, salt concentration, redox conditions, mixing ratio, and irradiation have all been examined as ways to improve the reaction conditions for the production of NPs. Chemical and physical factors determine the size and shape of NPs. In nanoparticle synthesis, the optimal metal ion concentration, temperature, and pH of the reaction mixture are important. Temperature, pH, substrate concentration, and exposure time to a substrate can all influence the rate of intracellular NPs formation and, as a result, the size of the NPs is affected.

Effects of plant extract percentage

The hydroxyl groups in plant extract are involved in the reduction process, therefore increasing the concentration of plant extract should result in a larger number of reductants. Previously, different amounts of plant extract were utilized, and the resulting NPs varied in size [72]. Sheny et al. investigated the influence of cashew leaf extract concentration on the production of Au and Ag NPs [73]. During the fabrication of NPs, an increase in plant extract percentage resulted in a broader SPR band, indicating an increase in particle size in contrast to Au, the SPR band of Ag nanoparticles tended to narrower as plant extract was increased. Furthermore, as more plant extract was added, a more symmetrical SPR band was detected. Although there is no clear explanation for how to plant extract affects nanoparticle formation, one of the parameters that control particle size is extract quantity regulation. Ahmad et al, investigated the morphology of Au-Ag NPs and found that as broth concentration was changed, hexagonal, triangular, and spherical shapes of synthesized NPs were formed. NPs developed spherical as broth concentrations increased [66]. When a 1:1 solution of plant broth and Au-Ag mixture was used, the particle size was determined to be the greatest (90 ± 2 nm), but when a 4:1 proportion was used, the particle size was the smallest (26 ± 2 nm). According to this study, an increase in broth concentration leads to a reduction in particle size. Surprisingly, the pH in each case remained consistent at 7.8.

Effect of precursor metal salt solution

Cu-Ni BMNPs were produced at two different concentrations, 1. 0 and 2. 0 mM solutions of silver nitrate + nickel nitrate hexahydrate salt, according to Akinsiku [40]. In 1. 0 and 2. 0 mM solutions, the SPR was observed at 327 and 330 nm, respectively. The reduced 2. 0 mM precursor had a higher absorption intensity. At 1. 0 mM concentration, a narrow SPR band was found in the absorption spectra, however, broadband was observed at higher concentrations, which could be due to anisotropic growth that resulted in larger particle formation. The observed broadband around 330 nm when the 2. 0 mM precursor solution was reduced suggests that Ni is highly increased on the surface of BMNPs, which is supported by TEM photographs. The effect of different reaction paramerters on morphology of synthesis of ZnO-Ag BMNPs, reported by Nadeem et al. (2019). In this study, ZnO-Ag BMNPs were synthesize utilising five different molarities of zinc acetate and silver nitrate, including (i) 0.5 M : 0.5 M, (ii) 0.1 M : 0.1 M, (iii) 0.5 M : 0.1 M, (iv) 0.1 M : 0.5 M, (v) 0.1 M : 0.5 M, and (vi) 1 M : 1 M (v) 0. 1M:0. 5M, and (vi) 1M:1M, with 50 ml leaf extract as reducing agent. Each set of BMNPs had a different form, ranging from plate like to sheet like, and a different size, ranging from 19.3 nm to 67.4 nm. Al-Haddad et al. (2020) investigated the effect of metal salt concentration on NPs yield at three different concentrations: 0.01 M, 0.05 M, and 0.10 M. Metal salts were prepared by mixing an equal volume of copper nitrate and silver nitrate solutions with the same molar concentration to synthesize BMNPs. The percentage yield of NPs was highest (80.1%) at the lowest bimetallic salt concentration and lowest at the highest salt concentration (36.2%).

The ionic ratio of bimetal salt

The ionic ratio was related to either core-shell or alloy bimetallic in the studies reviewed in this study. According to Sheny et al. at 1:2 ratios of Au to Ag [73], TEM images show electron density banding with a dark gold core and a light silver shell, indicating Au core–Ag shell NPs, and a particle size distribution histogram gives an average size of 6.5 nm, while at a 9:1 ionic ratio, TEM imaging showed homogenous electron density and in UV-Vis spectra agreement with the single SPR band observed. The development of alloy NPs was confirmed by the findings. The average particle size was 8 nm, according to their particle size histogram. This research reveals that alloy NPs have a little larger particle size than core-shell NPs. Sun et al. found that the Au^{3+}/Ag^{+} molar ratio in raw materials has a significant impact on not only the synthesis time but also the average size of generated Au–Ag alloy NPs [11]. At varying synthesis durations, TEM images showed size distributions of Au–Ag alloy NPs generated at the Au^{3+}/Ag^{+} molar ratio of 1:3.5. The resulting NPs are found to be sphere-like and have a constrained size distribution. The average size of Au–Ag alloy NPs steadily increases from 5.1 to 14.8 nm as the production progresses. Au–Ag alloy NPs with a size of 10.9 nm were generated at a molar ratio of 1:5 Au^{3+}/Ag^{+}.

The weight ratio of Au-Ag in Au-Ag alloy NPs was determined to be 1:5 for Au/Ag core-shell NPs and 3:1 for Au/Ag core-shell NPs by Leishangthem et al. [74]. TEM investigations revealed that synthesized NPs have a similar average diameter of 18 nm. Sharma et al. observed that Au-Ag (1:1) BMNPs were well diffused and had hexagonal and polygonal shapes [55]. The average particle size calculated is 16.04 nm. Particles in Au/Ag (3:1) BMNPs were predominantly spherical, although some triangular, hexagonal, and polyhedral shapes were also seen, with an average particle size of 28.06 nm. Particles of Au-Ag (1:3) BMNPs were mostly spherical, with some polyhedral in shape, with an average particle size of 44.37 nm. At a temperature of 130 °C. Silvestri et al. generated varied forms by varying the molar ratio of the bimetallic salt of Pd-Pt from 1:1, 1:2, and 2:1 [75]. Smaller NPswith a surface characterized by various, randomly-oriented Faces were produced when the molar ratio of bimetallic salt was 1:1. Figure 4 shows NPs with decahedral form when the molar ratio was altered to 2:1 and 1:2 (Pd-Pt).

Tien et al. [47] synthesized Ag-Mn nanoparticles using 2:1 and 1:1 ratios of silver nitrate and potassium permanganate solutions. Antibacterial activity has been observed in BMNPs that have been synthesized. The sample of (2Ag-1Mn) NPs was the most remarkable. The antibacterial activity of (2Ag-1Mn) NPs is attributed to its nanosize (3.3 nm) and Mn^{4+}, whereas (1Ag-1Mn)NPs have a little reduced antibacterial activity due to its larger nanosize and lower Mn^{4+} oxidation state in the sample, as demonstrated by TEM and XRD examination.

pH

To maintain particle homogeneity, particle size and shape must be controlled. The plant extract, as well as its pH, is one of the factors that might affect NPs morphology. The rate of NP production and morphology are affected by pH changes. At an alkaline pH, plant extract provides a significant number of functional groups that contribute to the reduction process and, as a result, generate a large number of NPs. The pH of leaves extract was regulated at three different values of pH, according to Al-Haddad et al. [28]. The BMNPs generated by the leaves extract at pH 3 were bigger than those produced at pH 7. The Cu-Ag BMNPs clustered together over the nucleation at low pH, resulting in bigger particles. Sharma et al. found that an alkaline pH is better for the production of Au-Ag BMNPs.

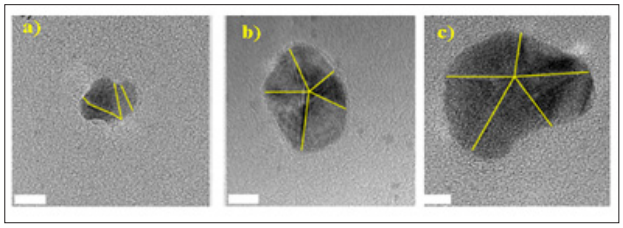

Figure 4: HR-TEM images of characteristic Pd-Pt nanoparticles synthesized with different molar ratios (a) 1:1, (b) 2:1, (c) 1:2. (Credit -Silvestri D, Wacławek S, K Ramakrishnan R, Venkateshaiah A, Krawczyk K, Padil VV, Sobel B, Černík M. The use of a biopolymer conjugate for an eco-friendly one-pot synthesis of palladium-platinum alloys. Polymers. 2019 Dec;11(12):1948)[75].

At pH 4, NPs are larger, with aggregation in some spherical and pentagonal shapes [55]. At pH 6, the average particle size was determined to be 21.31 nm, while NPs have a smaller average particle size of 13.20 nm. Particle fusion was also observed. Particles having triangular, spherical, and polyhedron shapesare well separated at pH 10. The investigation demonstrates that any of the NPs cannot be synthesized at an acidic pH. Korotkova et al. used an aqueous extract from the leaves of *Petroselinum crispum* in an acidic and alkaline medium to make bimetallic cobalt ferrite ($CoFe_2O_4$) NPs [76]. According to the UV-Vis spectra, in an acidic solution, had a little shoulder at 242 nm and a peak at 292 nm, whereas alkaline particles exhibited a plateau starting at 229 nm and a peak at 366 nm. The shape and size of $CoFe_2O_4$ bimetallic powders are also affected by the synthesis environment, according to SEM analysis: in an alkaline medium, the particles were hemispherical in size from 30 - 100 nm, whereas in a slightly acidic media (pH - 2), bigger particles with cut diamond were produced.

Reaction temperature

The temperature has a significant impact on the size, shape, and rate of NP production. At increasing temperatures, the generation of nucleation centers rises, which enhances the rate of biosynthesis. Song and Kim [77] have previously reported the formation of large particles during synthesis at high temperatures. They applied 95 °C to reduce Au and Ag ions into Au-Ag NPs, with particles ranging in size from 50 to 500 nm. The study also discovered a flaw in high-temperature synthesis. High-temperature NPs were not only more stable but also greater in size. However, as the concentration of plant extract increased, the particle size decreased. As a result, it was shown that while a higher reaction temperature produces more stable NPs, a high concentration of plant extract is necessary to obtain small particles. This could be due to the usage of insufficient amounts of plant extract. By varying the synthesis temperature from 130 to 150 °C, Silvestri et al. [75] were able to obtain different shapes. The sample produced at 150 °C with a 1:1 molar ratio (Pd-Pt) (Figure 5a) had a star-like structure, but lowering the synthesis temperature to 140 °C modified the NPs morphology to an octahedron (Figure 5b). A further drop in temperature to 130 °C resulted in the formation of smaller NPs with a surface characterized by a variety of randomly oriented faces (Figure 5c). According to Sharma et al. increasing the temperature enhances the yield of NPs and the rate of reduction [55]. The intensity of the peak increases as the temperature rises from 25 to 75 °C, but as the temperature rises more, the SPR band intensity decreases. Emam et al. investigated whether the effect reaction temperature will change the particle size of the as-synthesized Ag–Au bimetallic nanocomposite [78]. The obtained results revealed that increasing the reaction temperature resulted in a well dispersed and smaller sized bimetallic nanocomposite, which decreased from 6.5 nm at ambient temperature for sample S1 to 3.1 nm at 70 °C for sample S2. Fabrication of heterogeneous-sized bimetallic nanocomposite was obtained by the addition of alkali finally (S3) with average sizes of 6.6 and 14.9 nm (size distribution; 4 – 20 nm).

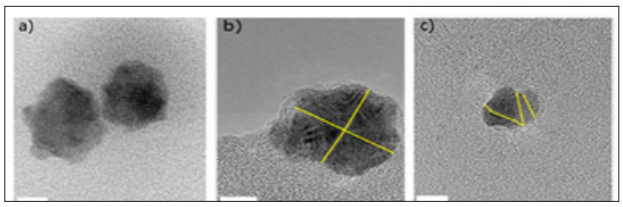

Figure 5: HR-TEM images of characteristic Pd/Pt nanoparticles synthesized with different temperatures (a) Pd/Pt 1:1 at 150 °C, (b) 1:1 at 140 °C, and (c) 1:1 at 130 °C. (Credit-Silvestri D, Wacławek S, K Ramakrishnan R, Venkateshaiah A, Krawczyk K, Padil VV, Sobel B, Černík M. The use of a biopolymer conjugate for an eco-friendly one-pot synthesis of palladium-platinum alloys. Polymers. 2019 Dec;11(12):1948).

Conclusion

Nanotechnology has straighten out a broad area of research and applications. Since conventional development methods of NPs are expensive and generate highly perilous products, it is critical to limit the risk of poisonous in the environment from the many chemicals used in physical and chemical methods. The benifits of green synthesis provide a long range of options for researchers to synthesize BMNPs from different plant parts. Persistently, we should motivate, the green synthesis of NPs from plant sources or genetically modified plant sources to synthesize NPs in a superior and more stable. The intensification of optical, biological, magnetic, electrical, mechanical, and catalytic properties is widely used for industrial scale-up and globally use in different sectors such as medicine, food, agriculture, industries, etc. This review focuses on the development of improved BMNPs, as well as the numerous factors that influence the synthesis of NPs and the various techniques are used to characterize them. Which will surely prove to be a boon to a society.

References

1. Singh M, Srivastava M, Kumar A, Pandey KD. 2019. Biosynthesis of nanoparticles and applications in agriculture In: Kumar A, Singh AK, Choudhary KK (eds) Role of Plant Growth Promoting Microorganisms in Sustainable Agriculture and Nanotechnology. Woodhead Publishing, Sawston. pp 199-217. https://doi.org/10.1016/B978-0-12-817004-5.00012-9
2. Sharma G, Kumar A, Sharma S, Naushad M, Dwivedi RP, et al. 2019. Novel development of nanoparticles to bimetallic nanoparticles and their composites: a review. *J King Saud Univ Sci* 31(2): 257-269. https://doi.org/10.1016/j.jksus.2017.06.012
3. Mortazavi SM, Khatami M, Sharifi I, Heli H, Kaykavousi K, et al. 2017. Bacterial biosynthesis of gold nanoparticles using *Salmonella enterica* subsp. *enterica* serovar Typhi isolated from blood and stool specimens of patients. *J Clust Sci* 28(5): 2997-3007. https://doi.org/10.1007/s10876-017-1267-0
4. Maghsoodi MR, Lajayer BA, HatamiM, Mirjalili MH. 2019. Challenges and opportunities of nanotechnology in plant-soil mediated systems: beneficial role, phytotoxicity, and phytoextraction. In: Ghorbanpour M, Wani SH (eds) Advances in Phytonanotechnology. Academic Press, Cambridge, pp 379-404. https://doi.org/10.1016/B978-0-12-815322-2.00018-3
5. Ghosh N, Singh R. 2020. Biogenic synthesis of bimetallic nanoparticles using cassia tora leaf extract. *Research Journal of Biotechnology* 15: 10.
6. Shah A, Khan SB, Asiri AM, Hussain H, Han C, et al. 2015. Synthesis, characterization, and application of Au–Ag alloy nanoparticles for the sensing of an environmental toxin, pyrene. *J Appl Electrochem* 45(5): 463-472. https://doi.org/10.1007/s10800-015-0807-2
7. Tomar RS, Chauhan PS, Shrivastava V. 2015. A critical review on nanoparticle synthesis: physicochemical v/s biological approach. *World journal of Pharmaceutical Research* 4(1): 595-620.
8. Behera A, Mittu B, Padhi S, Patra N, Singh J. 2020. Bimetallic nanoparticles: Green synthesis, applications, and future perspectives. In Abd-Elsalam (ed) Multifunctional Hybrid Nanomaterials for Sustainable Agri-Food and Ecosystems. Elsevier, Amsterdam. pp 639-682. https://doi.org/10.1016/B978-0-12-821354-4.00025-X
9. Alharthi FA, Alanazi HS, Alsyahi AA, Ahmad N. 2021. Hydrothermal synthesis, characterization and exploration of photocatalytic activities of polyoxometalate: Ni-$CoWO_4$ nanoparticles. *Crystals* 11(5): 456. https://doi.org/10.3390/cryst11050456
10. Song P, Lei Y, Hu X, Wang C, Wang J, Tang Y,et al. 2020. Rapid one-step synthesis of carbon-supported platinum–copper nanoparticles with enhanced electrocatalytic activity via microwave-assisted heating. *J Colloid Interface Sci* 574: 421-429. https://doi.org/10.1016/j.jcis.2020.04.041
11. Singaravelan R, Shanmugam M, Salam AA, Vasanthi P, Magesh M, et al. 2021. Electrochemical synthesis of γ-Cu_5 Zn_8 bimetallic nano alloy for efficient degradation of methyl orange dye and antimicrobial efficacy. *J Inorg Organomet Polym* 1-14. https://doi.org/10.1007/s10904-021-01989-0
12. Jwied DH, Nayef UM, Mutlak FA. 2021. Synthesis of C:Se (core:shell) nanoparticles via laser ablation on porous silicon for photodetector application. *Optik* 231: 166493. https://doi.org/10.1016/j.ijleo.2021.166493
13. Iqbal B, Laybourn A, Hamid A, Zaheer M. 2021. Size-controlled synthesis of spinel nickel ferrite nanorods by thermal decomposition of a bimetallic Fe/Ni-MOF. *Ceramics International* 47(9): 12433-12441. https://doi.org/10.1016/j.ceramint.2021.01.100
14. Zhao X, Wen J, Li L, Wang Y, Wang D, et al. 2019. Architecture design and applications of nanopatterned arrays based on colloidal lithography. *Journal of Applied Physics* 126(14): 141101. https://doi.org/10.1063/1.5120601
15. Boroumand Moghaddam A, Namvar F, Moniri M, Md Tahir P, Azizi S, et al. 2015. Nanoparticles biosynthesized by fungi and yeast: a review of their preparation, properties, and medical applications. *Molecules* 20(9): 16540-16565. https://doi.org/10.3390/molecules200916540
16. Ashishie PB, Anyama CA, Ayi AA, Oseghale CO, Adesuji ET, et al. 2018. Green synthesis of silver monometallic and copper-silver bimetallic nanoparticles using *Kigelia africana* fruit extract and evaluation of their antimicrobial activities. *International Journal of Physical Sciences* 13(3): 24-32. https://doi.org/10.5897/IJPS2017.4689
17. Karunakaran S, RamanujamS, Gurunathan B. 2018. Green synthesised iron and iron-based nanoparticle in environmental and biomedical application:–a review. *IET Nanobiotechnol* 12(8): 1003-1008. https://doi.org/10.1049/iet-nbt.2018.5048
18. Shedbalkar U, Singh R, Wadhwani S, Gaidhani S, Chopade BA. 2014. Microbial synthesis of gold nanoparticles: current status and future prospects. *Adv Colloid Interface Sci* 209: 40-48. https://doi.org/10.1016/j.cis.2013.12.011
19. Salem SS, Fouda A. 2021. Green synthesis of metallic nanoparticles and their prospective biotechnological applications: an overview. *Biol Trace Elem Res* 199(1): 344-370. https://doi.org/10.1007/s12011-020-02138-3
20. Hussain I, Singh NB, Singh A, Singh H, Singh SC. 2016. Green synthesis of nanoparticles and its potential application. *Biotechnol Lett* 38(4): 545-560. https://doi.org/10.1007/s10529-015-2026-7
21. Goshisht MK, Moudgil L, Rani M, Khullar P, Singh G, et al. 2014. Lysozyme complexes for the synthesis of functionalized biomaterials to understand protein–protein interactions and their biological applications. *J Phys Chem C* 118(48): 28207-28219. https://doi.org/10.1021/jp5078054

22. Zaleska-Medynska A, Marchelek M, DiakM, Grabowska E. 2016. Noble metal-based bimetallic nanoparticles: the effect of the structure on the optical, catalytic and photocatalytic properties. *Adv Colloid Interface Sci* 229: 80-107. https://doi.org/10.1016/j.cis.2015.12.008

23. Toshima N, Yonezawa T. 1998. Bimetallic nanoparticles—novel materials for chemical and physical applications. *New J Chem* 22(11): 1179-1201. https://doi.org/10.1039/A805753B

24. Kalishwaralal K, Deepak V, Ram Kumar Pandian S, Kottaisamy M, BarathmaniKanth S, et al. 2010. Biosynthesis of silver and gold nanoparticles using *Brevibacterium casei. Colloids Surf B Biointerfaces* 77(2): 257-262. https://doi.org/10.1016/j.colsurfb.2010.02.007

25. Riaz T, Mughal P, Shahzadi T, Shahid S, Abbasi MA. 2020. Green synthesis of silver nickel bimetallic nanoparticles using plant extract of *Salvadora persica* and evaluation of their various biological activities. *Mater Res Express* 6(12): 1250k3. https://doi.org/10.1088/2053-1591/ab74fc

26. Shankar SS, Rai A, Ahmad A, Sastry M. 2004. Rapid synthesis of Au, Ag, and bimetallic Au core–Ag shell nanoparticles using Neem (*Azadirachta indica*) leaf broth. *J Colloid Interface Sci* 275(2): 496-502. https://doi.org/10.1016/j.jcis.2004.03.003

27. Patra J K, Baek KH. 2014. Green nanobiotechnology: factors affecting synthesis and characterization techniques. *Journal of Nanomaterials* 2014: 417305. https://doi.org/10.1155/2014/417305

28. Al-Haddad J, Alzaabi F, Pal P, Rambabu K, Banat F. 2020. Green synthesis of bimetallic copper–silver nanoparticles and their application in catalytic and antibacterial activities. *Clean Techn Environ Policy* 22(1): 269-277. https://doi.org/10.1007/s10098-019-01765-2

29. Gopinath K, Sundaravadivelan C, Arumugam A. 2013. Green synthesis, characterization of silver, gold and bimetallic nanoparticles using bark extract of *Terminalia arjuna* and their larvicidal activity against malaria vector, *Anopheles stephensi*. *International Journal of Recent Scientific Research* 4(6): 904-910.

30. Danbature WL, Shehu Z, Yoro M, Adam MM. 2020. Nanolarvicidal effect of green synthesized Ag-Co bimetallic nanoparticles on *culex quinquefasciatus* mosquito. *Advances in Biological Chemistry* 10(1): 16-23. https://doi.org/10.4236/abc.2020.101002

31. Khatak S, Wadhwa N, Jain P. 2021. Monometallic zinc and bimetallic Cu-Zn nanoparticles synthesis using stem extracts of *Cissus quadrangularis* (Haddjod) and proneness as alternative antimicrobial agents. *Biosciences Biotechnology Research Asia* 17(4): 763-774. http://doi.org/10.13005/bbra/2881

32. Lamayi WD, Shehu Z, Mai AJ, Magaji B, Adam MM, et al. 2020. Green synthesis, characterization and larvicidal activity of Cu/Ni bimetallic nanoparticles using fruit extract of Palmyra palm. *International Journal of Chemistry and Materials Research* 8(1): 20-25. https://doi.org/10.18488/journal.64.2020.81.20.25

33. Masibi KK, Fayemi OE, Adekunle AS, Sherif ESM, Ebenso EE. 2020. Electrochemical determination of caffeine using bimetallic Au-Ag nanoparticles obtained from low- cost green synthesis. *Electroanalysis* 32(12): 2745-2755. https://doi.org/10.1002/elan.202060198

34. Bhattacharjee S, Habib F, Darwish N, Shanableh A. 2021. Iron sulfide nanoparticles prepared using date seed extract: Green synthesis, characterization and potential application for removal of ciprofloxacin and chromium. *Powder Technology* 380: 219-228. https://doi.org/10.1016/j.powtec.2020.11.055

35. Sundarrajan SK, Pottail L. 2021. Green synthesis of bimetallic Ag@Au nanoparticles with aqueous fruit latex extract of *Artocarpus heterophyllus* and their synergistic medicinal efficacies. *Appl Nanosci* 11(3): 971-981. https://doi.org/10.1007/s13204-020-01657-8

36. Suvarna AR, Shetty A, Anchan S, Kabeer N, Nayak S. 2020. *Cyclea peltata* leaf mediated green synthesized bimetallic nanoparticles exhibits methyl green dye degradation capability. *BioNanoSci* 10(3): 606-617. https://doi.org/10.1007/s12668-020-00739-9

37. Haleemkhan AA, Naseem B, Vardhini BV. 2015. Synthesis of nanoparticles from plant extracts. *Int J Mod Chem Appl Sci* 2(3): 195-203.

38. Rosbero TMS, Camacho DH. 2017. Green preparation and characterization of tentacle-like silver/copper nanoparticles for catalytic degradation of toxic chlorpyrifos in water. *J Environ Chem Eng* 5(3): 2524-2532. https://doi.org/10.1016/j.jece.2017.05.009

39. Canini A, Alesiani D, D Arcangelo G, Tagliatesta P. 2007. Gas chromatography–mass spectrometry analysis of phenolic compounds from *Carica papaya* L. leaf. *J Food Compost Anal* 20(7): 584-590. https://doi.org/10.1016/j.jfca.2007.03.009

40. Akinsiku AA, Ajanaku KO, Dare EO. 2019. Green synthesis of pseudo-cubic Ag/Ni bimetallic nanoparticles using *Senna occidentalis* leaf extract. *J. Phys.: Conf. Ser.* 1299(1): 012133.

41. Gopinath K, Kumaraguru S, Bhakyaraj K, Mohan S, Venkatesh KS, et al. Green synthesis of silver, gold and silver/gold bimetallic nanoparticles using the *Gloriosa superba* leaf extract and their antibacterial and antibiofilm activities. *Microb Pathog* 101: 1-11. https://doi.org/10.1016/j.micpath.2016.10.011

42. Verma V, Singh M, Singh PP, Singh J, Rawat M. 2020. Highly stable Au/Ag core–shell nanoparticles prepared via novel green approach for the abatement of nitro pollutants. *Micro & Nano Letters* 15(12): 822-825. https://doi.org/10.1049/mnl.2020.0275

43. Alti D, Veeramohan Rao M, Rao DN, Maurya R, Kalangi SK. 2020. Gold–silver bimetallic nanoparticles reduced with herbal leaf extracts induce ROS-mediated death in both promastigote and amastigote stages of *Leishmania donovani*. *ACS Omega* 5(26): 16238-16245. https://doi.org/10.1021/acsomega.0c02032

44. Lagashetty A, Ganiger SK, Shashidhar. 2019. Synthesis, characterization and antibacterial study of Ag–Au Bi-metallic nanocomposite by bioreduction using piper betle leaf extract. Heliyon 5(12): e02794. https://doi.org/10.1016/j.heliyon.2019.e02794

45. Luo F, Yang D, Chen Z, Megharaj M, Naidu R. 2016. One-step green synthesis of bimetallic Fe/Pd nanoparticles used to degrade Orange II. *J Hazard Mater* 303: 145-153. https://doi.org/10.1016/j.jhazmat.2015.10.034

46. Malik MA, Alshehri AA, Patel R. 2021. Facile one-pot green synthesis of Ag–Fe bimetallic nanoparticles and their catalytic capability for 4-nitrophenol reduction. *J Mater Res Technol* 12: 455-470. https://doi.org/10.1016/j.jmrt.2021.02.063

47. Van Tien H, Tri N, Anh NP, Nhi DM, Bich, LT, et al. 2020. Characterization and antibacterial activity of silver-manganese bimetallic nanoparticles biofabricated using *Arachis pintoi* extract. International *Int J Pharm Phytopharmacological Res* 10(1): 70-76.

48. Abdel-Aziz HM, Farag RS, Abdel-Gawad SA. 2019. Carbamazepine removal from aqueous solution by green synthesis zero-valent iron/Cu nanoparticles with *Ficus Benjamina* leaves' extract. *Int J Environ Res* 13(5): 843-852. https://doi.org/10.1007/s41742-019-00220-w

49. Adeyemi JO, Elemike EE, Onwudiwe DC, Singh M. 2019. Bio-inspired synthesis and cytotoxic evaluation of silver-gold bimetallic nanoparticles using Kei-Apple (*Dovyalis caffra*) fruits. *Inorg Chem Commun* 109: 107569. https://doi.org/10.1016/j.inoche.2019.107569

50. Adebayo AE, Oke AM, Lateef A, Oyatokun AA, Abisoye OD, et al. 2019. Biosynthesis of silver, gold and silver–gold alloy nanoparticles using *Persea americana* fruit peel aqueous extract for their biomedical properties. *Nanotechnol Environ Eng* 4: 13. https://doi.org/10.1007/s41204-019-0060-8

51. Shehu Z, Danbature WL, Muhammad MA. 2020. Ag/Ni bimetallic nanoparticles: eco-friendly synthesis, characterization and its bacteriocidal applications. *Jewel Journal of Medical Sciences* 1(1): 1-7.

52. Amina M, Al Musayeib NM, Alarfaj NA, El-Tohamy MF, Al-Hamoud GA. 2020. Antibacterial and immunomodulatory potentials of biosynthesized Ag, Au, Ag-Au bimetallic alloy nanoparticles us-

ing the *Asparagus racemosus* root extract. *Nanomaterials (Basel)* 10(12): 2453. https://doi.org/10.3390/nano10122453

53. Sharma D, Ledwani L, Kumar N, Mehrotra T, Pervaiz N, et al. 2021. An investigation of physicochemical and biological properties of rheum emodi-mediated bimetallic Ag–Cu nanoparticles. *Arab J Sci Eng* 46: 275-285. https://doi.org/10.1007/s13369-020-04641-0

54. Sarangapany S, Mohanty K. 2020. Facile green synthesis of magnetically separable Au–Pt@ TiO_2 nanocomposite for efficient catalytic reduction of organic pollutants and selective oxidation of glycerol. *J Alloys Compd* 830: 154636. https://doi.org/10.1016/j.jallcom.2020.154636

55. Sharma C, Ansari S, Ansari MS, Satsangee SP, Srivastava MM. 2020. Single-step green route synthesis of Au/Ag bimetallic nanoparticles using clove buds extract: Enhancement in antioxidant bio-efficacy and catalytic activity. *Mater Sci Eng C Mater Biol Appl* 116: 111153. https://doi.org/10.1016/j.msec.2020.111153

56. Cortés-Rojas DF, de Souza CR, Oliveira WP. 2014. Clove (*Syzygium aromaticum*): a precious spice. *Asian Pac J Trop Biomed* 4(2): 90-96. https://doi.org/10.1016/s2221-1691(14)60215-x

57. Jeevarathinam C, Solomon JS, Pandian G. 2019. *Crescentia alata* flower extract as reducing catalyst for green synthesis of au/ag bimetallic nano medicine and its antibacterial activities. *Journal of Applied Physical Science International* 11(4): 170-182. https://www.ikprress.org/index.php/JAPSI/article/view/4786

58. Venkateswara Rao A, Ashok B, Uma Mahesh M, Venkata Subbareddy G, Chandra Sekhar V, et al. 2019. Antibacterial cotton fabrics with in situ generated silver and copper bimetallic nanoparticles using red sanders powder extract as reducing agent. *Int J Polym Anal Char* 24(4): 346-354. https://doi.org/10.1080/1023666X.2019.1598631

59. Karthika V, Arumugam A, Gopinath K, Kaleeswarran P, Govindarajan M, et al. 2017. *Guazuma ulmifolia* bark-synthesized Ag, Au and Ag/Au alloy nanoparticles: Photocatalytic potential, DNA/protein interactions, anticancer activity and toxicity against 14 species of microbial pathogens. *J Photochem Photobiol B* 167: 189-199. https://doi.org/10.1016/j.jphotobiol.2017.01.008

60. Mishra K, Basavegowda N, Lee YR. 2015. Biosynthesis of Fe, Pd, and Fe–Pd bimetallic nanoparticles and their application as recyclable catalysts for [3+ 2] cycloaddition reaction: a comparative approach. *Catal Sci Technol* 5(5): 2612-2621. https://doi.org/10.1039/C5CY00099H

61. Gopalakrishnan R, Loganathan B, Raghu K. 2015. Green synthesis of Au–Ag bimetallic nanocomposites using *Silybum marianum* seed extract and their application as a catalyst. *RSC Adv* 5(40): 31691-31699. https://doi.org/10.1039/C5RA03571F

62. Sharma M, Yadav S, Ganesh N, Srivastava MM, Srivastava S. 2019. Biofabrication and characterization of flavonoid-loaded Ag, Au, Au–Ag bimetallic nanoparticles using seed extract of the plant *Madhuca longifolia* for the enhancement in wound healing bio-efficacy. *Prog Biomater* 8: 51-63. https://doi.org/10.1007/s40204-019-0110-0

63. Mallikarjuna K, Bathula C, Reddy GD, Shrestha NK, Kim H, et al. 2019. Au-Pd bimetallic nanoparticles embedded highly porous Fenugreek polysaccharide based micro networks for catalytic applications. *Int J Biol Macromol* 126: 352-358. https://doi.org/10.1016/j.ijbiomac.2018.12.137

64. Kumari MM, Jacob J, Philip D. 2015. Green synthesis and applications of Au–Ag bimetallic nanoparticles. *Spectrochim Acta A Mol Biomol Spectrosc* 137: 185-192. https://doi.org/10.1016/j.saa.2014.08.079

65. Newase S, Bankar AV. 2017. Synthesis of bio-inspired Ag–Au nanocomposite and its anti-biofilm efficacy. *Bull Mater Sci* 40: 157-162. https://doi.org/10.1007/s12034-017-1363-7

66. Ahmad N, Sharma AK, Sharma S, Khan I, Sharma DK, et al. 2019. Biosynthesized composites of Au-Ag nanoparticles using *Trapa* peel extract induced ROS-mediated p53 independent apoptosis in cancer cells. *Drug Chem Toxicol* 42(1): 43-53. https://doi.org/10.1080/01480545.2018.1463241

67. Ravikumar KVG, Sudakaran SV, Ravichandran K, Pulimi M, Natarajan C, et al. 2019. Green synthesis of NiFe nano particles using *Punica granatum* peel extract for tetracycline removal. *Journal of Cleaner Production* 210: 767-776. https://doi.org/10.1016/j.jclepro.2018.11.108

68. Wicaksono WP, Kadja GT, Amalia D, Uyun L, Rini WP, et al. 2020. A green synthesis of gold–palladium core–shell nanoparticles using orange peel extract through two-step reduction method and its formaldehyde colorimetric sensing performance. *Nano-Structures & Nano-Objects* 24: 100535. https://doi.org/10.1016/j.nanoso.2020.100535

69. Shankar S, Rhim JW. 2015. Amino acid mediated synthesis of silver nanoparticles and preparation of antimicrobial agar/silver nanoparticles composite films. *Carbohydr Polym* 130: 353-363. https://doi.org/10.1016/j.carbpol.2015.05.018

70. Anandalakshmi K, Venugobal J, Ramasamy V. 2016. Characterization of silver nanoparticles by green synthesis method using *Pedalium murex* leaf extract and their antibacterial activity. *Appl Nanosci* 6(3): 399-408. https://doi.org/10.1007/s13204-015-0449-z

71. Mohamad NA, Jai J, Arham NA, Hadi A. 2013. A short review on the synthesis of bimetallic nanoparticles using plant extract. In: 2013 IEEE International Conference On Control System, Computing And Engineering. IEEE, pp 334-339. https://doi.org/10.1109/ICCSCE.2013.6719985

72. Sheny DS, Mathew J, Philip D. 2011. Phytosynthesis of Au, Ag and Au–Ag bimetallic nanoparticles using aqueous extract and dried leaf of *Anacardium occidentale*. *Spectrochim Acta A Mol Biomol Spectrosc* 79(1): 254-262. https://doi.org/10.1016/j.saa.2011.02.051

73. Nadeem A, Naz S, Ali JS, Mannan A, Zia M. 2019. Synthesis, characterization and biological activities of monometallic and bimetallic nanoparticles using *Mirabilis jalapa* leaf extract. *Biotechnol Rep* 22: e00338. https://doi.org/10.1016/j.btre.2019.e00338

74. Leishangthem D, Yumkhaibam MAK, Henam PS, Nagarajan S. 2018. An insight into the effect of composition for enhance catalytic performance of biogenic Au/Ag bimetallic nanoparticles. *J Phys Org Chem* 31(6): e3815. https://doi.org/10.1002/poc.3815

75. Silvestri D, Wacławek S, Ramakrishnan RK, Venkateshaiah A, Krawczyk K, et al. 2019. The use of a biopolymer conjugate for an eco-friendly one-pot synthesis of palladium-platinum alloys. *Polymers Basel* 11(12): 1948. https://doi.org/10.3390/polym11121948

76. Korotkova AM, Polivanova OB, Gavrish IA, Lebedev SV. 2019. Biological synthesis of bimetallic nanoparticles of cobalt ferrate $CoFe_2O_4$ in an aqueous extract of *Petroselinum crispum*. *Earth Environ Sci* 341: 012178. https://doi.org/10.1088/1755-1315/341/1/012178

77. Song JY, Kim BS. 2008. Biological synthesis of bimetallic Au/Ag nanoparticles using Persimmon (*Diopyros kaki*) leaf extract. *Korean J Chem Eng* 25(4): 808-811. https://doi.org/10.1007/s11814-008-0133-z

78. Emam HE. 2019. Arabic gum as bio-synthesizer for Ag–Au bimetallic nanocomposite using seed-mediated growth technique and its biological efficacy. *J Polym Environ* 27: 210-223. https://doi.org/10.1007/s10924-018-1331-3

79. Anuradha ChS, Bai GS, Datla S. 2020. Plant mediated green synthesis of novel bimetallic nanoparticles: characterization and investigation of photocatalytic activity for degradation of malachite green dye. *International Journal of Research and Analytical Reviews* 7(1): 404-416.

80. Weng X, Guo M, Luo F, Chen Z. 2017. One-step green synthesis of bimetallic Fe/Ni nanoparticles by eucalyptus leaf extract: biomolecules identification, characterization and catalytic activity. *Chemical Engineering Journal* 308: 904-911. https://doi.org/10.1016/j.cej.2016.09.134

81. Merugu R, Nayak B, Chitturi K L, Misra P K. 2021. Bimetallic silver and copper nanoparticles synthesis, characterization and biological

evaluation using aqueous leaf extracts of *Majorana hortensis*. *Materials Today: Proceedings* 44(Part 1): 2454-2458. https://doi.org/10.1016/j.matpr.2020.12.516

82. Abbasi BH, Zaka M, Hashmi SS, Khan Z. 2018. Biogenic synthesis of Au, Ag and Au–Ag alloy nanoparticles using *Cannabis sativa* leaf extract. *IET Nanobiotechnology* 12(3): 277-284. https://doi.org/10.1049/iet-nbt.2017.0169

83. Minal SP, Prakash S. 2020. Laboratory analysis of AuPd bimetallic nanoparticles synthesized with *Citrus limon* leaf extract and its efficacy on mosquito larvae and non-target organisms. *Scientific Reports* 10(1): 1-13. https://doi.org/10.1038/s41598-020-78662-y

84. Oladipo AO, Iku SI, Ntwasa M, Nkambule TT, Mamba BB, et al. 2020. Doxorubicin conjugated hydrophilic AuPt bimetallic nanoparticles fabricated from *Phragmites australis*: characterization and cytotoxic activity against human cancer cells. *J Drug Deliv Sci Technol* 57: 101749. https://doi.org/10.1016/j.jddst.2020.101749

85. Elemike EE, Onwudiwe DC, Nundkumar N, Singh M, Iyekowa O. 2019. Green synthesis of Ag, Au and Ag-Au bimetallic nanoparticles using *Stigmaphyllon ovatum* leaf extract and their *in vitro* anticancer potential. *Materials Letters* 243: 148-152. https://doi.org/10.1016/j.matlet.2019.02.049

86. Shehu Z, Danbature WL, Magaji B, Adam MM, Bunu MA, et al. 2020. Green synthesis and nanotoxicity assay of Copper-Cobalt bimetallic nanoparticles as a novel nanolarvicide for mosquito larvae management. *The International Journal of Biotechnology* 9(2): 99-104. https://doi.org/10.18488/journal.57.2020.92.99.104

87. Merugu R, Garimella S, Velamakanni R, Vuppugalla P, Chitturi KL, et al. 2021. Synthesis, characterization and antimicrobial activity of bimetallic silver and copper nanoparticles using fruit pulp aqueous extracts of *Moringa oleifera*. *Materials Today: Proceedings* 44: 153-156. https://doi.org/10.1016/j.matpr.2020.08.549

88. Sun L, Yin Y, Lv P, Su W, Zhang L. 2018. Green controllable synthesis of Au–Ag alloy nanoparticles using Chinese wolfberry fruit extract and their tunable photocatalytic activity. *RSC Advances* 8(8): 3964-3973. https://doi.org/10.1039/C7RA13650A

89. Singh R, Nawale L, Arkile M, Wadhwani S, Shedbalkar U, et al. 2016. Phytogenic silver, gold, and bimetallic nanoparticles as novel antitubercular agents. *Int J Nanomedicine* 11: 1889-1897. https://doi.org/10.2147/IJN.S102488

90. Ismail M, Khan MI, Khan SA, Qayum M, Khan MA, et al. 2018. Green synthesis of antibacterial bimetallic Ag–Cu nanoparticles for catalytic reduction of persistent organic pollutants. *J Mater Sci Mater Electron* 29(24): 20840-20855. https://doi.org/10.1007/s10854-018-0227-2

91. Khatak S, Wadhwa N, Jain P. 2021. Monometallic zinc and bimetallic Cu-Zn nanoparticles synthesis using stem extracts of *Cissus quadrangularis* (Haddjod) and Proneness as alternative antimicrobial agents. *Biosciences Biotechnology Research Asia* 17(4): 763-774. https://doi.org/10.13005/bbra/2881

92. Nasrollahzadeh M, Sajadi SM, Rostami-Vartooni A, Bagherzadeh M. 2015. Green synthesis of Pd/CuO nanoparticles by *Theobroma cacao* L. seeds extract and their catalytic performance for the reduction of 4-nitrophenol and phosphine-free Heck coupling reaction under aerobic conditions. *J Colloid Interface Sci* 448: 106-113. https://doi.org/10.1016/j.jcis.2015.02.009

93. Ghosh S, Nitnavare R, Dewle A, Tomar GB, Chippalkatti R, et al. 2015. Novel platinum–palladium bimetallic nanoparticles synthesized by *Dioscorea bulbifera*: anticancer and antioxidant activities. *Int J Nanomedicin*e 10: 7477. https://doi.org/10.2147/IJN.S91579